A unified framework for exploring hysteresis between charge and discharge processes in supercapacitors

Corentin Renais, Charles Cougnon

A unified framework for exploring hysteresis between charge and discharge processes in supercapacitors

Corentin Rénais,[a] and Charles Cougnon[*,a]

[a]*Université d'Angers, CNRS UMR 6200, Laboratoire MOLTECH-Anjou, 2 bd Lavoisier, 49045 ANGERS cedex, France.*

charles.cougnon@univ-angers.fr, Fax: +33 (0)2 41 73 54 05

Abstract

In supercapacitor technology, the determination of the largest voltage range useable for the charge storage is a key parameter to optimize their energy. For this purpose, "acceptable" coulombic and energy efficiencies are commonly used as cut-off values to delineate a safe operational potential window in opening-window charge-discharge experiments. Because of the arbitrariness of such an approach, attempts have been made over the past three decades to rationalize the determination of the stability window, but differentiate between capacitive and faradaic currents remains challenging. Assuming that it's better to examine what is lost during the charge period to investigate the degradation of electrochemical interfaces, part of the problem is that we have not the correct perspective on stability with coulombic and energy efficiencies, since they give an indication of the way in which performance are retained during the charge process, as they represent the capacitive fractions of the measured quantities. Here, we propose a new formalism based on non-capacitive fractions to focus on what is lost during the charge period, in order to place the heterogeneous kinetics of the electrochemical degradation processes at the center of the debate on stability of the electrode-electrolyte interfaces in supercapacitors.

Introduction

As the electrochemical stability in supercapacitors cannot be extracted from the notion of operational potential window, which itself is linked to their energy [1-4], stability must be regarded as an evolving concept, constantly shifting in step with the changes in technology and stated needs. With the prospect of the electrochemical stationary storage for securing the energy transition, these considerations are becoming more important than ever, so that storage systems could face a paradigm shift in the approach to their stability [5-8]. Conceptually, the important thing in determining the stability window is to ensure that optimum performance be secured over a long-time period [9-11]. Only then will energy storage systems be seen as a viable option, making them both competitive and attractive compared to other energy sources such as fossil fuels. Unfortunately, the absence of standardized methods to reliably evaluate performance and stability of electrochemical storage systems makes challenging the comparison between storage technologies and acts as a significant brake on the research in this area [12-17]. For these reasons, a realistic stability criterion is urgently required in order to conduct objective evaluation of performance and to close the gap between laboratory and large-scale industrial production.

Initially based on the coulombic efficiency (CE) [18-22], there is a general consensus that the energy efficiency (EE) should be preferred for exploring the stability of high-energy and high-power storage technologies [23], because of its impact on the charging cost and, by implication, its economic impact on the levelized cost of storage, excluding capital, operation and maintenance costs [24]. From an academic perspective, the reason for this new interest is because EE is the most sensitive parameter due to the cumulative effects of coulombic and voltage efficiencies ($\mathrm{EE} = \mathrm{CE} \times \mathrm{VE}$) [25]. At the same time however, it cannot be concluded, just on the basis of EE, that a poor charge-discharge efficiency results from a resistive problem or an electrochemical degradation [26]. To answer this question, we must have a complete overview of all the metrics used for discussing the various aspects of the charge-discharge efficiency, and also a fine knowledge of their interdependencies [27]. However, even though CE and VE are identified as being responsible for EE [28-30], only an individual analysis of these parameters has been done to date, ignoring their possible interdependence.

With this approach, the stability window is approximated by gradually increasing the full charge voltage in window-opening charge-discharge experiments, with evaluation, at each stage, of CE, VE and EE. Noted that such a determination remains arbitrary, as it is based on the choice of a cut-off value for CE or EE [31]. The direct consequence is that the evaluation of the stability window is totally disconnected from the interfacial dynamics, being unable of distinguishing between electrode kinetics and electrostatic charging at the interface [32]. Here, a new formalism is presented for exploring the stability of electrode-electrolyte interfaces, taking into consideration the heterogeneous kinetics by examining the non-capacitive fractions of the measured quantities for the charge period instead of the capacitive ones as with CE, VE and EE. Within such a unified framework, the impact of capacitive and faradaic processes on the energy losses have been distinguished by introducing the concept of "degradation core energy", and a new realistic stability criterion is proposed, which allows to put the interfacial kinetics at the center of the determination of the stability window. This has involved the introduction of "breaking potentials" as fatal potential limits that can be approached but not exceeded, otherwise the interface will suffer from severe damages. Importantly, such "breaking potentials" are not determined arbitrarily by the experimenter, but imposed by electrode kinetics, so that we propose that they could advantageously replace the commonly used potential limits, which are unable to distinguish faradaic current from capacitive current [33].

Experimental section

Fabrication of supercapacitor electrodes. The electrodes tested were prepared by mixing the YP80F activated carbon with poly(vinilydene fluoride) (PVDF) and graphite (from Superior graphite) with a ratio of 80:10:10 (w:w:w) in a small volume of tetrahydrofuran (THF) until a homogeneous carbon ink was obtained. Next, a small volume of carbon ink was spread on a platinum disk of 18 mm diameter used as current collector. After drying at 65 °C for one night, thin-film electrodes of 2.7 mg ± 0.3 mg were obtained with equivalent series resistance (ESR) of 0.5 Ω ± 0.05 Ω for ensuring approximately the same ohmic drop in charge-discharge experiments.

Cell assembling and testing. In all studies, carbon-based supercapacitor electrodes having the same mass were assembled in a symmetrical two-electrode and three-electrode cell configurations. The electrodes were separated by glass fiber paper impregnated with about 200 mg of 1 M Bu_4NBF_4/propylene carbonate (PC). For the three-electrode configuration, a silver wire was used as a quasi-reference electrode potential. Electrochemical cells were assembled and tested in a glove box under galvanostatic conditions at 1 A g^{-1} and 10 A g^{-1} (for the long-term cycle tests).

Results and discussion

Presentation of the formalism

A comprehensive description of the charge-discharge reversibility can be summed up by a joint examination of the coulombic, voltage and energy efficiencies (CE, VE and EE) [25-27]. These metrics are defined by the set of Eqs. (1), where Q_{ch} and Q_{dis} represent the electric charge stored and delivered during a charge-discharge cycle, $\overline{V_{\mathrm{ch}}}$ and $\overline{V_{\mathrm{dis}}}$ represent the average charge and discharge voltage, while ξ_{ch} and ξ_{dis} represent the amount of energy calculated by integrating the charge and the discharge curves. Fig. 1 gives a graphic representation of these metrics and parameters on which they depend. Noted that the charge-discharge curve showed in Fig. 1 is for a three-electrode cell configuration, so that, in these conditions, VE is most correctly identified as a potential efficiency, and $\overline{V_{\mathrm{ch}}}$ and $\overline{V_{\mathrm{dis}}}$ are strictly speaking the average charge and discharge electrode potentials. This is an opportunity to reinforce the importance of exploring the stability of electrochemical charge storage systems in a two-electrode cell configuration, because this is misleading to associate the notion of energy with that of electrode potential, as the evaluation of the stability window from a single electrode analysis can be different to that obtained from the packed cell when a limiting electrode exists [32]. In the present study, we are first exploring the stability in a three-electrode cell configuration to evaluate the individual responsibility of each electrode and then, in a second stage, the evaluation of a realistic stability window will be made in a two-electrode cell configuration.

$$\begin{cases} \mathrm{CE} = \dfrac{Q_{\mathrm{dis}}}{Q_{\mathrm{ch}}} \\ \mathrm{VE} = \dfrac{\overline{V_{\mathrm{dis}}}}{\overline{V_{\mathrm{ch}}}} = \dfrac{\dfrac{1}{Q_{\mathrm{dis}}}\int_{Q_{\mathrm{ch}}}^{(Q_{\mathrm{ch}}-Q_{\mathrm{dis}})} V\mathrm{d}q}{\dfrac{1}{Q_{\mathrm{ch}}}\int_{0}^{Q_{\mathrm{ch}}} V\mathrm{d}q} \\ \mathrm{EE} = \dfrac{\xi_{\mathrm{dis}}}{\xi_{\mathrm{ch}}} = \dfrac{\int_{Q_{\mathrm{ch}}}^{(Q_{\mathrm{ch}}-Q_{\mathrm{dis}})} V\mathrm{d}q}{\int_{0}^{Q_{\mathrm{ch}}} V\mathrm{d}q} \end{cases} \quad (1)$$

The interrelationship between these metrics is given by Eq. (2), making the energy efficiency the most sensitive indicator to the degradation of the electrode-electrolyte interface, due to the cumulative effects of CE and VE:

$$\mathrm{EE} = \frac{Q_{\mathrm{dis}} \times \overline{V_{\mathrm{dis}}}}{Q_{\mathrm{ch}} \times \overline{V_{\mathrm{ch}}}} = \mathrm{CE} \times \mathrm{VE} \quad (2)$$

In a pioneering work [18,19], Xu and R. Jow propose to handle CE as a fraction defined by the ratio of the charge hysteresis ΔQ to the delivered charge:

$$\mathrm{R_{CE}} = \frac{Q_{\mathrm{ch}} - Q_{\mathrm{dis}}}{Q_{\mathrm{dis}}} = \frac{\Delta Q}{Q_{\mathrm{dis}}} = \frac{(1 - \mathrm{CE})}{\mathrm{CE}} \quad (3)$$

In spite of its complex nature [35], ΔQ is most commonly identified with the irreversible faradaic charge consumed to degrade the electrode-electrolyte interface, so that the fraction $\mathrm{R_{CE}}$ can be regarded as a faradaic fraction. It should be noted here that the “CE” subscript is just a reminder that this fraction is related to the coulombic efficiency. Such a faradaic fraction has the merit of giving a quantitative estimate of the electrochemical degradation in a manner commensurate with the available amount of electricity during the discharge period. Here, we propose to define voltage and energy hysteresis ratios modelled on that of $\mathrm{R_{CE}}$ for handling voltage and energy efficiencies:

$$\begin{cases} \mathrm{R_{VE}} = \dfrac{\overline{V_{\mathrm{ch}}} - \overline{V_{\mathrm{dis}}}}{\overline{V_{\mathrm{dis}}}} = \dfrac{\Delta \overline{V}}{\overline{V_{\mathrm{dis}}}} = \dfrac{(1-\mathrm{VE})}{\mathrm{VE}} \\ \mathrm{R_{EE}} = \dfrac{\xi_{\mathrm{ch}} - \xi_{\mathrm{dis}}}{\xi_{\mathrm{dis}}} = \dfrac{\Delta \xi}{\xi_{\mathrm{dis}}} = \dfrac{(1-\mathrm{EE})}{\mathrm{EE}} \end{cases} \quad (4)$$

At this stage, it is important to note that CE, VE and EE represent the capacitive fractions of Q_{ch}, $\overline{V_{\mathrm{ch}}}$ and ξ_{ch}, while $(1-\mathrm{CE})$, $(1-\mathrm{VE})$ and $(1-\mathrm{EE})$ are the corresponding non-capacitive fractions. In this perspective, $\mathrm{R_{CE}}$, $\mathrm{R_{VE}}$ and $\mathrm{R_{EE}}$ are indicative of the extent to which capacitive and non-capacitive fractions are balanced together. With this unified framework, we have the possibility to fully understand the charge-discharge efficiency, by exploring the stability of electrode-electrolyte interfaces from all perspectives (i.e. from the perspective of what is preserved, or in term of what is lost during a complete charge-discharge cycle).

The interrelationship between hysteresis ratios can be easily deduced to Eq. (2):

$$\mathrm{R_{EE}} = \frac{\Delta \xi}{\xi_{\mathrm{dis}}} = \mathrm{R_{CE}} + \mathrm{R_{VE}} + \mathrm{R_{CE}} \times \mathrm{R_{VE}} \quad (5)$$

Eq. (5) implies that $\Delta \xi$ can be decomposed into three parts, corresponding to the three light grey rectangle areas in Fig. 1. In this developed expression for $\mathrm{R_{EE}}$, the individual impact of $\mathrm{R_{CE}}$ on the energy lost is because the amount of electricity delivered during the discharge is ΔQ less than the one consumed during the charge period, and the individual impact of $\mathrm{R_{VE}}$ is due to the fact that, during the discharge period, the amount of electricity is delivered at an average potential decreased by $\Delta \overline{V}$, compared to the average charge potential. In other words, the part of the energy lost expressed in ξ_{dis} unit that is represented by $\mathrm{R_{CE}} + \mathrm{R_{VE}}$ stems from the fact that the extra charge ΔQ is not stored in the double-layer and that it is consumed at extreme potentials in absolute terms, where its energy cost is maximum. Ultimately, the discussion above can be boiled down to the simple statement that the total energy lost by charging the double-layer depends to the energy of the double-layer. The last term $\mathrm{R_{CE}} \times \mathrm{R_{VE}}$ in the developed expression of $\mathrm{R_{EE}}$ refers to the elemental amount of energy $\Delta Q \times \Delta\overline{V}$ standardized by ξ_{dis} (Fig. 1). From an analytical point of view, this elemental amount of energy is equivalent to the energy linked with a charge ΔQ consumed by an electrolyzer operating at an applied potential equal to $\Delta\overline{V}$, so that it can be approximated to the part of $\Delta\xi$ that is converted in chemical energy, assuming that ΔQ is faradaic by nature. Summing up the above, $\mathrm{R_{CE}} + \mathrm{R_{VE}}$ reflects the impact of the energy of the double-layer on $\Delta\xi$, while $\mathrm{R_{CE}} \times \mathrm{R_{VE}}$ reflects the impact of the interfacial kinetics, regardless of the energy of the double-layer at which the electrochemical degradation occurs.

At this stage, it is of interest to note that Eq. (5) can be rewritten in a form similar to that of Eq. (2):

$$(1 - \mathrm{EE}) = \frac{\Delta\xi}{\Delta Q \times \Delta\overline{V}} \times (1 - \mathrm{CE}) \times (1 - \mathrm{VE}) \quad (6)$$

The same analytical form for Eqs. (2) and (6) and the fact that the sum of their respective right and left members is equal to unity, imply that capacitive and non-capacitive fractions are complementary fractions that jointly represent Q_{ch}, $\overline{V_{\mathrm{ch}}}$ and ξ_{ch}, so that these two equations are complementary approaches to explore the stability of the electrode-electrolyte interface. Eq. (2) examines the extent to which performances for energy storage are preserved during the charge process, while Eq. (6) is concerned with the importance of the charge, potential and energy losses during the charge process.

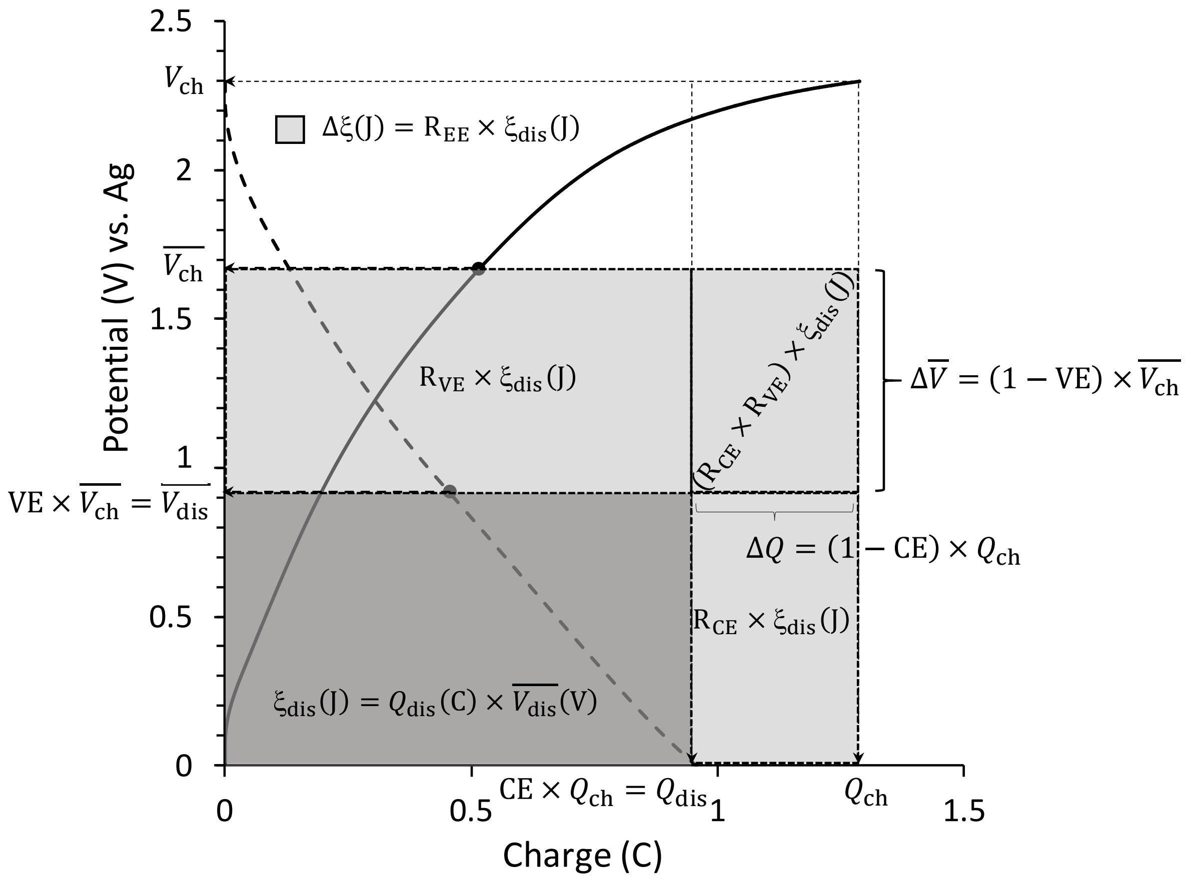

Fig. 1. Graphic illustration of the formalism used to explore hysteresis in the charge-discharge profile of a carbon-based supercapacitor electrode during galvanostatic cycling to 2.3 V at 1 A g^{-1} in 1 M Bu_4NBF_4/PC electrolyte.

Concept of breaking potentials

Generally speaking, it results from Eq. (5) that the amount of energy lost during the charge process is exceeding the sum of the individual impact of R_{CE} and R_{VE} by a term related to their product. Here, it is worth noting that R_{CE} and R_{VE} are closely interlinked, since where ΔQ is produced, a growing increase of the average charge potential (or the average charge voltage, depending to the cell configuration used) results due to the consumption of the extra degradation charge at both ends of the stability window where its energy cost is the most important. This connection enabled the product $R_{CE} \times R_{VE}$ to be identified as a coupling product between CE and VE. Consequently, the anodic and cathodic potentials at which a growing increase in $R_{CE} \times R_{VE}$ starts, denote potentials where the effect of ΔQ in exacerbating $\Delta\overline{V}$ cannot be ignored. In this way, based on the relative importance of this coupling product on the total energy lost, the potential window can be divided in two domains where $\mathrm{R_{EE}} \approx \mathrm{R_{CE}} + \mathrm{R_{VE}}$, reflecting the individual impact of ΔQ and $\Delta\overline{V}$ on $\Delta\xi$, and where $\mathrm{R_{EE}} > \mathrm{R_{CE}} + \mathrm{R_{VE}}$, reflecting the cooperative impact of ΔQ and $\Delta\overline{V}$ on $\Delta\xi$ (Fig. 2a). The first potential domain can be assimilated to a purely capacitive domain as the average charge and discharge potentials vary linearly (Fig. 2b). This is because where the coupling product is negligible, ΔQ has a very small value (vide infra). Noted that, in this potential domain, $\overline{V_{\mathrm{dis}}}$ is less than the geometric mean of the full charge potential, $\frac{1}{2}V_{\mathrm{ch}}$, while $\overline{V_{\mathrm{ch}}}$ is more important due to the ohmic drop. In contrast, where the coupling product has a significant impact on $\Delta\xi$, ΔQ has an increasing responsibility for $\Delta\overline{V}$, so that $\overline{V_{\mathrm{ch}}}$ becomes increasingly important, while $\overline{V_{\mathrm{dis}}}$ is growing more slowly and even declining.

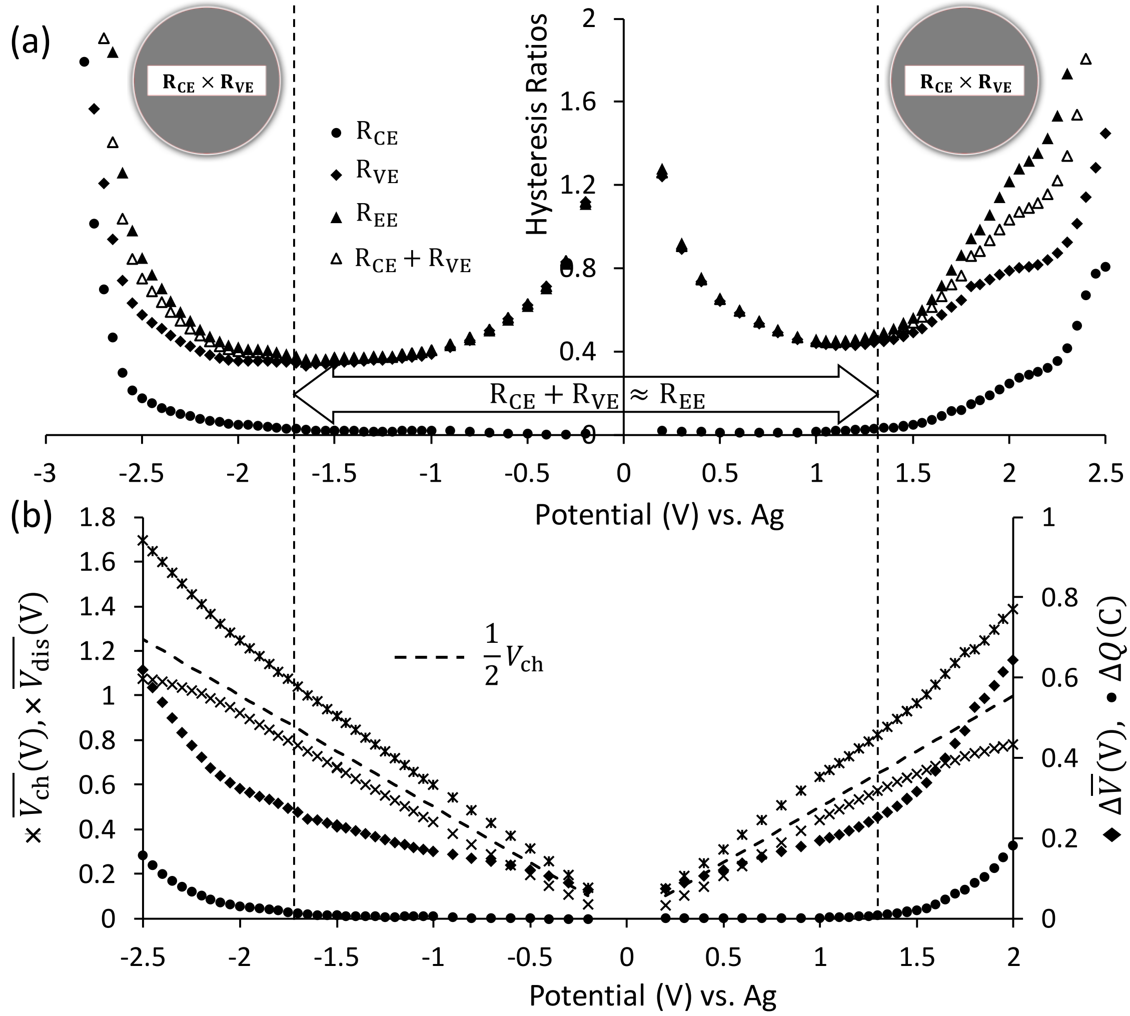

Fig. 2. (a) Evolution of R_{CE}, R_{VE} and R_{EE} with electrode potentials calculated from a series of galvanostatic cycles at 1 A g^{-1} in 1 M Bu_4NBF_4/PC from 0 V to variable vertex potentials. (b) Evidence of the coupling between charge and voltage losses and its impact on the electrification at the interface. Dotted lines are for the evolution of the geometric mean of the full charge potential, $\frac{1}{2}V_{ch}$.

Observing that the hysteresis ratios R_{CE} and R_{VE} increased in an accelerated manner when exceeding anodic and cathodic potential limits at both ends of the stability window, because of the Arrhenius rate form of electrochemical processes, it exists critical negative and positive potentials at which the product $R_{CE} \times R_{VE}$ becomes rapidly significant, allowing to clearly separate negative and positive safe potential domains beyond which ΔQ has an aggravating impact on $\Delta\overline{V}$. Such critical potential limits can be identified with breaking potentials and can be regarded as fatal cathodic and anodic potential limits beyond which the total energy lost is increasingly impacted by the faradaic charge consumed in electrochemical degradation processes. At this stage, it is important to note that breaking potentials are imposed by electrode kinetics, since the way in which ΔQ impacts $\Delta\overline{V}$ is closely related to how the faradaic current increases with the overpotential, in contrast to the well-known potential limits widely used for determining the safe potential window and arbitrarily set. As a result of the above, breaking potentials have the potentiality to provide a precise and realistic identification of the stability window as they delineate the largest potential window in which the electric charge is efficiently stored in the electrochemical double-layer, including an "acceptable" loss of charge having a negligible impact on $\Delta\overline{V}$. Such a determination of the stability window corresponds to an optimal use of supercapacitors, because where the coupling product $\mathrm{R_{CE}} \times \mathrm{R_{VE}}$ has a significant responsibility in the total energy lost, the energy efficiency of the charge-discharge cycle rapidly decreased, thus becoming "uneconomic".

How precisely should breaking potentials be determined?

It follows from the above that breaking potentials could advantageously replace the commonly used potential limits, which are unable of distinguishing between faradaic current and capacitive current, provided, however, that a practical criterion could be found for securing their determination. With the understanding that breaking potentials correspond to negative and positive potentials at which ΔQ has an aggravating effect on $\Delta\overline{V}$, the potential dependence of the relative importance of $\Delta Q \times \Delta\overline{V}$ on $\Delta\xi$ can be used for determining their values. From a practical point of view, a one-to-one relationship between hysteresis ratios and non-capacitive quantities can be obtained:

$$\frac{\Delta Q \times \Delta\overline{V}}{\Delta\xi} = \frac{\mathrm{R_{CE}} \times \mathrm{R_{VE}}}{\mathrm{R_{EE}}} \qquad (7)$$

Noted that the equation above is equivalent to Eq. (6) since ΔQ, $\Delta\overline{V}$ and $\Delta\xi$ can be identified with the non-capacitive parts of Q_{ch}, $\overline{V_{\mathrm{ch}}}$ and ξ_{ch}. As a consequence, the coupling product $\mathrm{R_{CE}} \times \mathrm{R_{VE}}$ standardized with respect to $\mathrm{R_{EE}}$ reflects the relative importance of $\Delta Q \times \Delta\overline{V}$ on $\Delta\xi$ that is indicative of the impact of the electrode kinetics, so that its evolution with potential can be used as a metric for the determination of the breaking potentials theorized above. In the rest of this work, the elemental amount of energy $\Delta Q \times \Delta\overline{V}$ will be identified in a degradation core energy $\Delta\xi_{\mathrm{core}}$ as a reminder that it is independent of the energy of the electrochemical double-layer.

Fig. 3a shows a series of galvanostatic charges-discharge curves in a three-electrode cell and illustrates the evolution of $\Delta\xi_{\mathrm{core}}$, materialized by hatched rectangular blocks, as the anodic and cathodic electrode potentials increase. For better demonstration, the discharge curve in dotted line was superimposed on each charge curve and the average charge and discharge potentials were marked with symbols.

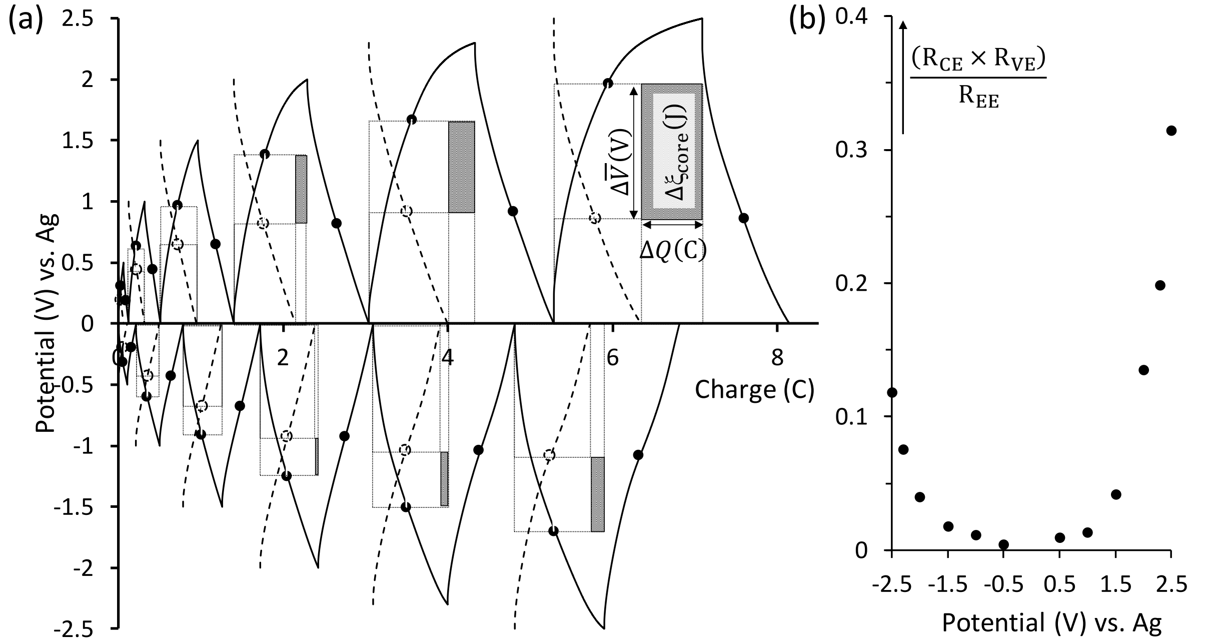

Fig. 3 (a) Evolution of the degradation core energy for a series of galvanostatic charge-discharge cycles in a three-electrode cell at 1 A g^{-1} in 1 M Bu_4NBF_4/PC with electrode potential at the full-charge state rising from 1 V to 2.5 V vs. Ag in absolute terms. (b) Evolution of the normalized coupling factor with the electrode potential.

When supercapacitor electrodes work in a stable potential window where the degradation is negligible, $\Delta\xi_{\mathrm{core}}$remains insignificant, implying that the energy lost is almost exclusively due to the capacitive storage through the ohmic drop. In that case, it can be verified in Fig. 3a that R_{EE} is equivalent to R_{VE}, $\Delta\xi$ being just ohmic in nature [36]. Beyond the safe potential window, degradation starts and $\overline{V_{\mathrm{ch}}}$ and $\overline{V_{\mathrm{dis}}}$ are more and more far apart from each other as

ΔQ increases, making $\Delta\xi_{\text{core}}$ a growing fraction of $\Delta\xi$. This is evidence of the impact of ΔQ on $\Delta\overline{V}$. Noted that the sudden increase in $\mathrm{R_{CE}} \times \mathrm{R_{VE}}$ relatively to $\mathrm{R_{EE}}$ makes the normalized coupling product a sensitive indicator to identify precisely the breaking potentials (Fig. 3b). Importantly, breaking potentials are not set arbitrarily by the experimenter, as with methods based on cut-off criteria, but imposed by the heterogeneous kinetics of the electrochemical degradation processes, which is a pre-requisite for determining a realistic stability domain of the electrode-electrolyte interface.

Breaking voltage as realistic limit for the stability window

To ensure that the normalized coupling product can be used as stability criterion, it makes sense to explore the stability in a two-electrode cell configuration to ensure that a breaking voltage corresponds. In the same time, it is crucial to verify that such a breaking voltage can be reached without alteration of the stability over long time. So, long-term repetitive galvanostatic charge-discharge cycling were achieved in a two-electrode cell at different voltages, in the prospect of exploring the deterioration with time. In order to make it possible to accumulate a large number of cycles, galvanostatic experiments were achieved at 10 A g^{-1}. This first require determining the breaking voltage in these new conditions. Fig. 4a shows charge-discharge cycles with cell voltage rising from 1 V to 4 V. The hatched rectangular surfaces correspond to the degradation core energy and the average charge and discharge voltages are marked with black dots. As a result, Fig. 4b presents the evolution of the normalized coupling product over the 2 to 4 V voltage range. Its rapid increase allows the breaking voltage to be located at around 3.2 V, in good agreement with published results [37].

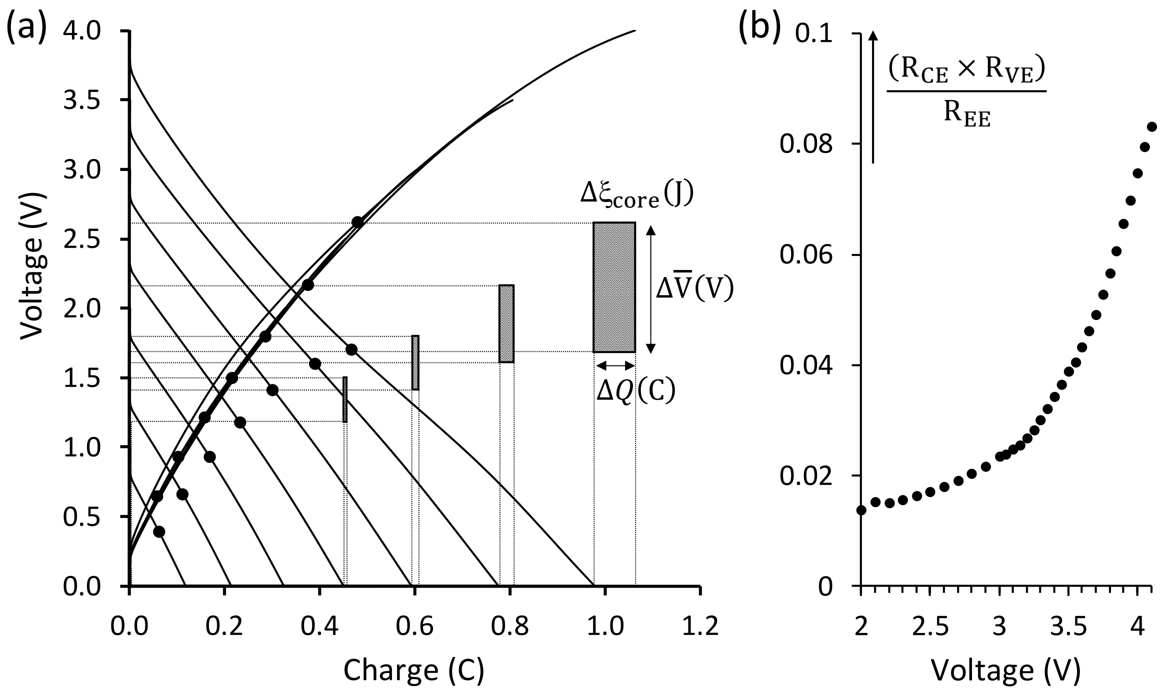

Fig. 4. (a) Evolution of $\Delta\xi_{core}$ for galvanostatic charge-discharge cycles obtained in a two-electrode cell at 10 A g^{-1} in 1 M Bu_4NBF_4/PC with full-charge voltage rising from 1 V to 4 V. (b) Evolution of the normalized coupling product in the 2 to 4 V voltage range.

In order to verify that severe damage to the interface will result by crossing the breaking voltage, repetitive charge-discharge cycles for long time was achieved at cell voltages higher and lesser than the breaking voltage. Fig. 5 presents the evolution of Q_{dis} over 10,000 cycles for cell voltages comprised between 2.7 V and 3.5 V. Two distinct behaviours were observed as the cell voltage exceed or not the breaking voltage. For cell voltages not exceeding 3.2 V, a slow and steady decrease of Q_{dis} was obtained with a charge-loss rate of ca. 0.6% at each 1000-cycle interval (Fig. 5 inset). Beyond 3.2 V, Q_{dis} decreases in an accelerated manner as the cell voltage exceeds the breaking value. Remarkably, the rate of loss of the specific charge delivered is increasing sharply immediately after that the breaking voltage is exceeding, implying that the breaking voltage sets an upper limit which can be approached but not exceeded.

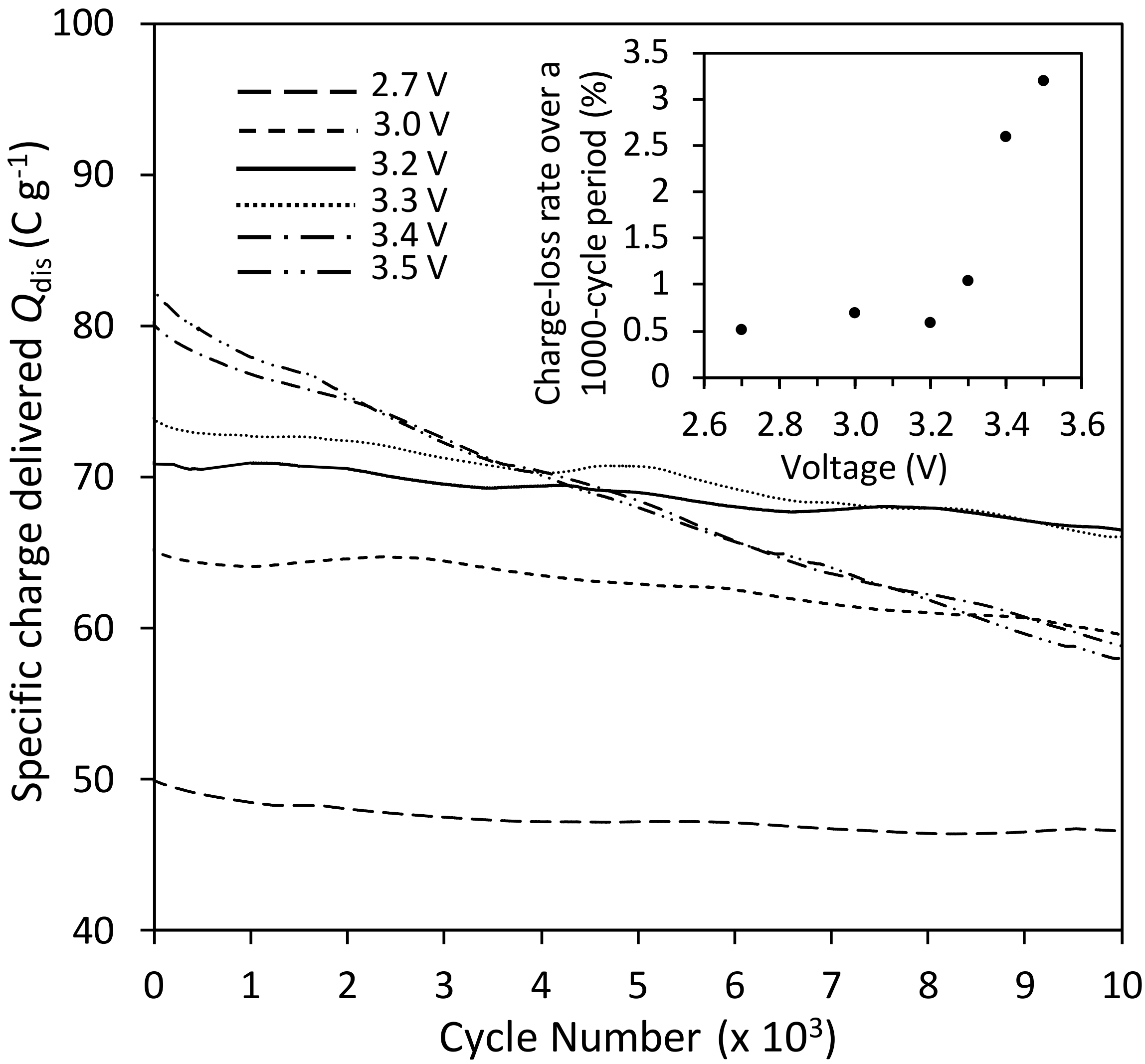

Fig. 5 . Evolution of the delivered specific charge for a long-time cycling at 10 A g^{-1} with different full-charge voltage comprised between 2.7 V and 3.5 V. Inset shows the evolution of the average charge-loss rate at each 1000 cycles.

This critical change is due to the aggravating effect of ΔQ on $\Delta\overline{V}$ as demonstrated by the evolution of CE and VE at the end of the repetitive charge-discharge tests (Fig. 6a). When exceeding 3.2 V, the extra charge ΔQ consumed in the degradation processes resulted in increased the part of the cell voltage that does not contribute to the storage $\Delta\overline{V}$. This is because the faradaic charge consumed at the end of the cell voltage produces a growing increase of the average charge voltage, while the evolution of the average discharge voltage is increasingly low because a growing fraction of the electric charge consumed at extreme voltage is not accumulated in the double-layer. As an illustration, Fig. 6b demonstrates that the double-layer is efficiently electrified up to 3.2 V, producing a linear increase of Q_{dis}, $\overline{V_{\mathrm{dis}}}$

and ξ_{dis}, while exceeding this value the supercapacitor is subjected to ageing conditions, resulting in a decrease of Q_{dis} and ξ_{dis}.

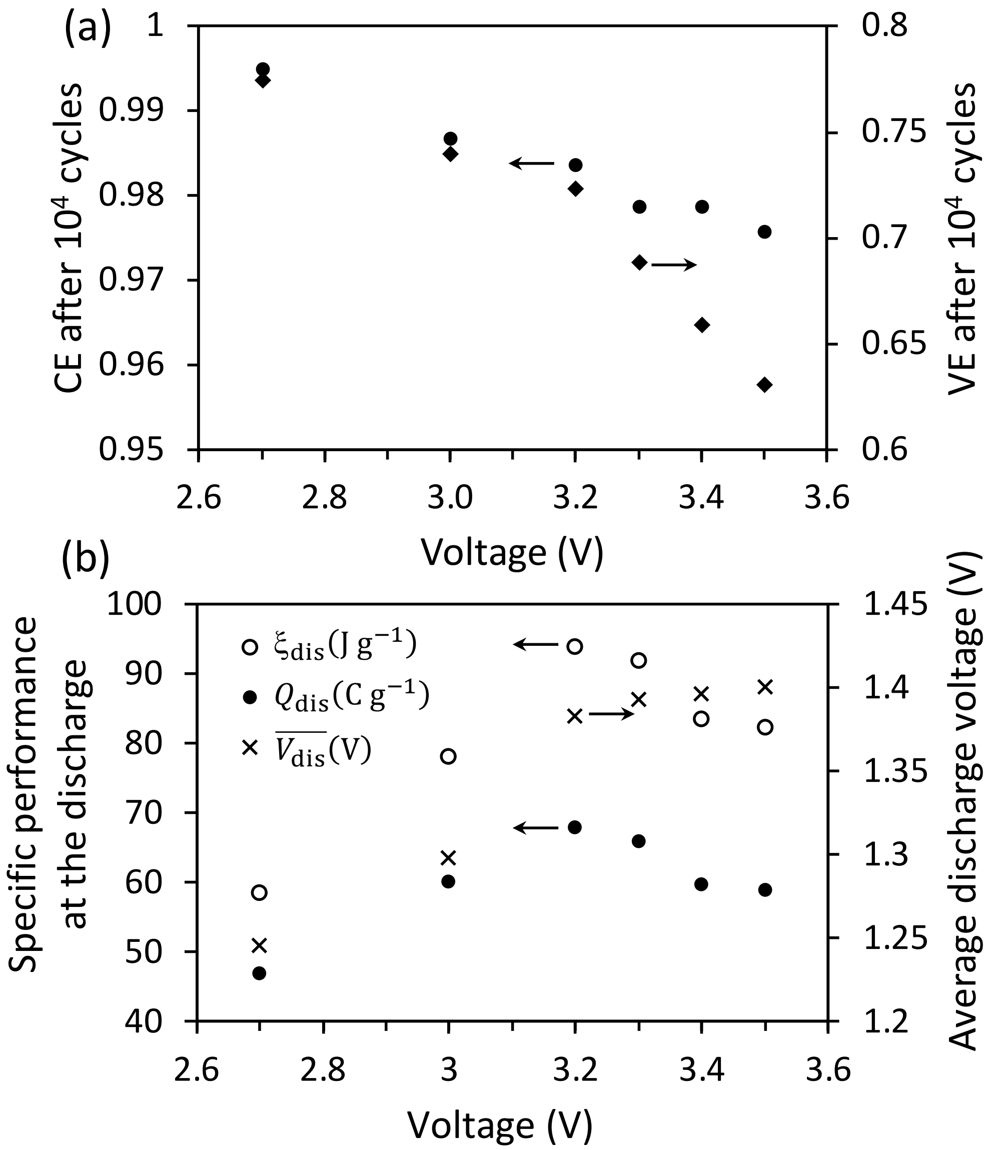

Fig. 6. (a) Evolution of CE and VE at the end of the repetitive charge-discharge tests presented in Fig. 5. (b) Quality of the capacitive energy storage for cell voltages lower and higher than the breaking voltage.

So, the breaking voltage can be regarded as a fatal potential limit at which the impact of the electrochemical degradation on the energy lost starts to expand in importance relative to the capacitive storage. A maximum value for the energy density at the breaking voltage is the direct consequence. Assuming that 2.7 V is a typical nominal voltage for carbon-based supercapacitors working in these conditions [38], an energy gain of ca. 50% is obtained by working at the breaking voltage.

Remarkably, the breaking voltage is not arbitrarily defined by the experimenter, but its value is determined by the interfacial dynamics on which the importance of the impact of ΔQ on $\Delta\overline{V}$ depends. The result is that the normalized coupling product $(\mathrm{R_{CE}} \times \mathrm{R_{VE}})/\mathrm{R_{EE}}$ can serve as stability criterion for exploring the stability of electrochemical capacitors with two consequences that a realistic metrics for determining the stability window is obtained, and that the coupling product has the potentiality to be used as a predictive tool to guide the rational choice of electrolytes for maximizing the energy density based on kinetics considerations. Here, it has been demonstrated that the new stability criterion allows for expanding the stability window until an optimal energy density is obtained with the guarantee of a stability window secured in voltage and time.

Conclusion

This work is laying the foundation for a unified framework for exploring the charge-discharge hysteresis problem in supercapacitors. The charge, voltage and energy hysteresis $\left(\Delta Q, \Delta\overline{V} \text{ and } \Delta\xi\right)$ are the functionalities of this new formalism and their transformation into hysteresis ratios $\mathrm{R_{CE}}$, $\mathrm{R_{VE}}$ and $\mathrm{R_{EE}}$, is the rule based on which the formalism is derived. Importantly, the interdependency between charge and voltage hysteresis, emerging from a coupling product $\mathrm{R_{CE}} \times \mathrm{R_{VE}}$, allows to put the interfacial kinetics in the center of the evaluation of the interface stability. The result is the possibility to distinguish between the impact of capacitive and faradaic processes on the energy lost and to isolate the responsibility of the electrode kinetics in the energy efficiency by introducing the concept of "degradation core energy". As a consequence, a new realistic stability criterion that gives the relative importance of $\Delta\xi_{\mathrm{core}}$ on $\Delta\xi$ allows to determine breaking potentials as fatal potential limits beyond which the interface undergoes severe damage, because of an aggravating effect of ΔQ on $\Delta\overline{V}$. Repetitive charge-discharge tests over a long-time period demonstrate that the breaking voltage can be approached, but not exceeded, constituting the largest potential range useable for optimum charge storage in the double-layer secured in voltage and time.

Acknowledgements

This work was supported by the Centre National de la Recherche Scientifique (CNRS-France).

References

[1] P. Simon, Y. Gogotsi, Nat. Mater. 19 (**2020)** 1151-1163.

[2] Q. Gao, L. Demarconnay, E. Raymundo-Piñero, F. Béguin, Energy Environ. Sci. 5 (2012) 9611-9617.

[3] M. Yu, Y. Lu, H. Zheng, X. Lu, Chem. Eur. J. 24 (2018) 3639-3649.

[4] S. Zheng, Z.-S. Wu, S. Wang, H. Xiao, F. Zhou, C. Sun, X. Bao, H.-M. Cheng, Energy Storage Mater. 6 (2017) 70-97.

[5] J.B. Goodenough, Energy Environ. Sci. 7 (2014) 14-18.

[6] T. Liu, Y. Zhang, Z. Jiang, X. Zeng, J. Ji, Z. Li, X. Gao, M. Sun, Z. Lin, M. Ling, J. Zheng, C. Liang, Energy Environ. Sci. 12 (2019) 1512-1533.

[7] Z. Yang, J. Zhang, M.C.W. Kintner-Meyer, X. Lu, D. Choi, J.P. Lemmon, J. Liu, Chem. Rev. 111 (2011) 3577-3613.

[8] G.F. Frate, L. Ferrari, U. Desideri, Renew. Energ. 163 (2021) 1754-1772.

[9] P. Ruschhaupt, S. Pohlmann, A. Varzi, S. Passerini, Batteries Supercaps 3 (2020) 698-707.

[10] D. Weingarth, A. Foelske-Schmitz, R. Kötz, J. Power Sources 225 (2013) 84-88.

[11] T. Zhang, B. Fuchs, M. Secchiaroli, M. Wohlfahrt-Mehrens, S. Dsoke, Electrochimi Acta 218 (2016) 163-173.

[12] T.S. Mathis, N. Kurra, X. Wang, D. Pinto, P. Simon, Y. Gogotsi, Adv. Energy Mater. 9 (2019) 1902007.

[13] A. Noori, M.F. El-Kady, M.S. Rahmanifar, R.B. Kaner, M.F. Mousavi, Chem. Soc. Rev. 48 (2019) 1272-1341.

[14] A. Eftekhari, ACS Sustainable Chem. Eng. 7 (2019) 3688-3691.

[15] J. Zhao, A.F. Burke, Adv. Energy Mater. 11 (2021) 2002192.

[16] Y. Gogotsi, P. Simon, Science 334 (2011) 917-918.

[17] N.R. Chodankar, H.D. Pham, A.K. Nanjundan, J.F.S. Fernando, K. Jayaramulu, D. Golberg, Y.K Han, D.P. Dubal, Small 16 (2020) 2002806.

[18] K. Xu, S.P. Ding, T.R. Jow, J. Electrochem. Soc. 146 (1999) 4172-4178.

[19] K. Xu, M.S. Ding, T.R. Jow, Electrochimi. Acta 46 (2001) 1823-1827.

[20] D. Weingarth, H. Noh, A. Foelske-Schmitz, A. Wokaun, R.Kötz, Electrochim Acta 103 (2013) 119-124.

[21] T. Zhang, B. Fuchs, M. Secchiaroli, M. Wohlfahrt-Mehrens, S. Dsoke, Electrochim. Acta 218 (2016) 163-173.

[22] J. Xiao, Q. Li, Y. Bi, M. Cai, B. Dunn, T. Glossmann, J. Liu, T. Osaka, R. Sugiura, B. Wu, J. Yang, J.G. Zhang, M.S. Whittingham, Nat Energy 5 (2020) 561-568.

[23] A. Eftekhari, Sustain. 1 (2017) 2053-2060.

[24] I. Pawel, Energy Procedia 46 (2014) 68-67.

[25] P. Meister, H. Jia, J. Li, R. Kloepsch, M. Winter, T. Placke, Chem. Mater. 28 (2016) 7203-7217.

[26] R. Lu, A. Yang, Y. Xue, L. Xu, C. Zhu, World Electr. Veh. J. 4 (2010) 9-13.

[27] C. Cougnon, Electrochem. Commun. 120 (2020) 106832.

[28] A. Laheäär, P. Przygocki, Q. Abbas, F. Béguin, Electrochem. Commun. 60 (2015) 21-25.

[29] B. Pillay J. Newman, J. Electrochem. Soc. 143 (1996) 1806-1814.

[30] M. Pohl, I. Tallo, A. Jänes, T. Romann, E. Lust, J. Power Sources 402 (2018) 53-61.

[31] M.C.G. Santos, G.G. Silva, R. Santamaría, P.F.R. Ortega, R.L. Lavall, J. Phys. Chem. C 123 (2019) 8541-8549.

[32] M. Bahdanchyk, M. Hashempour, A. Vicenzo, Electrochim. Acta 332 (2020) 135503.

[33] N. De Vos, C. Maton, C. V. Stevens, ChemElectroChem 1 (2014) 1258-1270.

[34] M.P.S. Mousavi, A.J. Dittmer, B.E. Wilson, J. Hu, A. Stein, P. Bühlmann, J. Electrochem. Soc. 162 (2015) A2250-A2258.

[35] C. Cougnon, Electrochim. Acta 371 (2021) 137788.

[36] Y. Zhong, J. Zhang, G. Li, A. Liu, Internat. Conf. Power System Technol. (2006) 1.

[37] F. Zheng, Y. Li, X. Wang, Electrochim. Acta 276 (2018) 343-351.

[38] M. Hahn, A. Würsig, R. Gallay, P. Novák, R. Kötz, Electrochem. Commun. 7 (2005) 925-930.